Downlink Non-Orthogonal Multiple Access (NOMA) Constellation Rotation

Jian Zhang*, Xin Wang*, Tsuyoshi Hasegawa†, and Tokuro Kubo†
*Fujitsu Research and Development Center Co., Ltd., Beijing P.R. China
†Fujitsu Laboratories Ltd., Japan
Email: zhangjian1288@cn.fujitsu.com

***Abstract*—The non-orthogonal multiple access (NOMA) technique or more generally the non-orthogonal principle is a crucial component for the next generation cellular system. For two-user downlink NOMA, the constellations of near and far users are superposed for transmission, and maximum likelihood (ML) or successive interference cancellation (SIC) receiver is used for reception. In this paper, we aim to further enhance the link-level performance for NOMA with ML receiver. A method of NOMA constellation rotation is proposed where the constellations are respectively rotated before superposition so as to exploit signal space diversity. The symbol error rate (SER) upper bounds for both near and far users are derived and used for rotation angle optimization. Within this framework, we show the best we can do in terms of enhancing the performance for a particular user (either near or far). Simulation results have verified the effectiveness of our proposed method. It can be observed that there is performance gain for one user while almost no negative impact on the other user.**

I. Introduction

Higher system spectrum efficiency is always the target of cellular mobile communications. As the 5th generation (5G) wireless system, International Mobile Telecommunications 2020 (IMT-2020) is expected to support a 1000 times higher area traffic capacity and a 3∼5 times higher spectrum efficiency compared with Long Term Evolution Advanced (LTE-A) [1]. To meet this high demand, non-orthogonality has been accepted as a new design principle on top of the prevalent orthogonal criteria. The theoretical basis is that non-orthogonal techniques are proved to be able to achieve the whole capacity region for both broadcast (downlink) and multiple access (uplink) channels [2].

Non-orthogonal multiple access (NOMA) is one flavor of non-orthogonal techniques. For downlink NOMA [3], signals for different users are superposed and transmitted. For two-user cases, they are distinguished as near and far users depending on distances from the transmitter or equivalently channel qualities in terms of signal-to-noise ratio (SNR). Successive interference cancellation (SIC) or maximum likelihood (ML) receiver can be used by near user. For SIC, near user first decodes far user's data, and then cancels it to proceed its own decoding. For ML, near user directly performs decoding based on the composite constellation formed by superposition. Compared with ML, codeword-level (CW) SIC requires higher complexity and larger signaling overhead. Far user usually does not decode near user's data, but it can always perform decoding by treating near user's data as noise.

Deployment of NOMA in cellular systems has demonstrated great potential for enhancing spectrum efficiency, e.g., system-level results in [3] show gains in both cell average and cell edge throughput. NOMA modulation [4]-[8], power allocation, user scheduling [9] [10], and combination with multiple-input multiple-output (MIMO) and coordinated multipoint (CoMP) [11] [12] are popular research topics. As for NOMA modulation which is the focus of this paper, different bit labelling and receiving methods have been investigated in literatures. It is proposed in [4] that a composite constellation following Gray mapping (called Gray-mapping NOMA hereafter) is used for transmission and near user performs ML detection instead of CW SIC. Similar proposals are also under discussion within 3rd Generation Partnership Project (3GPP) [5]-[7]. For near user, Gray-mapping NOMA outperforms conventional NOMA (non-Gray-mapping) when using ML receiver [5] [6], and ML detection achieves similar performance with that of CW SIC [4]-[7]. These are encouraging results w.r.t. enhancing near user performance, and also receiver complexity and signaling overhead will be reduced if SIC is not used. As for the impact of NOMA modulation on far user, it is proposed in [8] that far user performs ML detection based on the composite constellation rather than treating near user's data as noise. The gain comes from the fact that far user is aided with a priori information on interference caused by near user.

The interest of this paper is NOMA modulation, and we focus on enhancing NOMA link-level performance. A method of NOMA constellation rotation is proposed based on the theory of signal space diversity [13]. The modulated signals for near and far users are rotated respectively before superposition, and interleaving is performed next. Assuming ML detection, symbol error rate (SER) upper bounds for both users are derived and used to optimize rotation angles. The optimization can be performed towards either near or far user, and we show the best performance a particular user can achieve. The proposed method is compared with aforementioned state-of-the-art techniques using Gray-mapping NOMA and ML receivers. Simulation results show performance gain for near (far) user while almost no performance loss for far (near) user.

The rest of this paper is organized as follows. Section II gives a general description on NOMA. In Section III, the proposed NOMA constellation rotation method is introduced and rotation optimization is elaborated. Simulation results are given in Section IV. Finally Section V concludes this paper.

978-1-5090-1701-0/16/$31.00 ©2016 IEEE

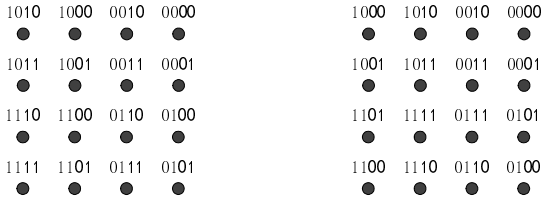

a) Conventional NOMA b) Gray-mapping NOMA

Fig. 1. Conventional NOMA v.s. Gray-mapping NOMA.

II. NOMA System model

Without loss of generality, a two-user NOMA model is assumed with both transmitter and receiver equipped with single antenna. The transmitted signal is given as

$$x = \sqrt{E}\left(\sqrt{\rho_a}a + \sqrt{\rho_b}b\right), \tag{1}$$

where a, b are normalized symbols for near and far users respectively, E is the total power, and ρ_a, ρ_b are power ratios with larger power allocated to far user. Defining $z = \sqrt{\rho_a}a + \sqrt{\rho_b}b$ as a symbol from the composite constellation, the signal received by either near or far user can be given as

$$r = h\sqrt{E}z + \eta, \tag{2}$$

where h denotes small-scale fading with $E\{|h|^2\} = 1$, and η is equivalent noise with large-scale fading absorbed into it. Although a universal formulation is used, near and far users can be distinguished by assuming different noise powers (i.e., different large-scale fading). The post-processed signal is

$$y = rh^*/|h| = |h|\sqrt{E}z + n, \tag{3}$$

where $n = \eta h^*/|h|$, and $|h|$ is defined as the channel gain. Assuming QPSK for both users, Fig. 1 compares conventional and Gray-mapping NOMA constellations. For the composite constellation, the first and latter two bits are for far and near users respectively. For Gray mapping, constellation points with minimum Euclidean distances have only one bit difference. Gray-mapping NOMA with ML detection based on the composite constellation has been proven advantageous for both near and far users [4]-[8], and is thus the starting point for our research. In this paper, ML detection will be always interpreted as ML detection based on the composite constellation.

III. NOMA constellation rotation

In this section, a method of NOMA constellation rotation is proposed. Processing at transmitter and receiver is introduced and we provide a way to optimize rotation angles.

A. Transmitter processing

Within orthogonal frequency division multiplexing (OFDM) framework, the transmitter of NOMA constellation rotation is given in Fig. 2. Channel coding and Gray mapping are denoted as "Code" and "Gray" respectively. After modulation "MOD", constellation is rotated in "ROT" followed by power allocation "POW". The output are superposed and then interleaved in "Interlv". Finally resource element (RE) mapping and OFDM

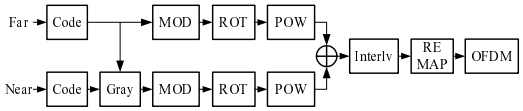

Fig. 2. Transmitter structure of NOMA constellation rotation.

modulation are performed. Constellation rotation and interleaving are newly introduced on top of Gray-mapping NOMA.

1) Constellation rotation: Constellation rotation transforms the superposed signal in (1) into the following form

$$x = \sqrt{E}\left(\sqrt{\rho_a}ae^{-j\theta_a} + \sqrt{\rho_b}be^{-j\theta_b}\right), \tag{4}$$

where θ_a and θ_b denote rotation angles for near and far users respectively. It is revealed in [13] that a type of diversity called signal space diversity (SSD) can be obtained by rotating the modulated symbols by a certain angle. Due to superposition of two symbols in NOMA, two independent rotation angles are used in this paper to preserve full degrees of freedom.

2) Real and imaginary part interleaving: Real and imaginary parts of a sequence of x will be interleaved to exploit diversity gain. The rationale is phase rotation $(a_R + ja_I)e^{-j\theta} = (a_R\cos\theta + a_I\sin\theta) - j(a_R\sin\theta - a_I\cos\theta)$ makes a_R, a_I replicated in both real and imaginary parts. Diversity w.r.t a_R, a_I can be obtained if real and imaginary parts are sent through independent channels. The same applies to (4), where both real and imaginary parts of x contain replica real and imaginary components of a and b. Thereby, diversity can be obtained by interleaving real and imaginary parts of x. This is an additional diversity on top of bit-level interleaving before modulation.

B. Receiver processing

Let $z = \sqrt{\rho_a}ae^{-j\theta_a} + \sqrt{\rho_b}be^{-j\theta_b}$ denote a symbol from the rotated composite constellation. By de-interleaving the post-processed signals as in (3), we have

$$y_{\Re} = h_R\sqrt{E}z_{\Re} + n_{\Re}, \tag{5}$$

$$y_{\Im} = h_I\sqrt{E}z_{\Im} + n_{\Im}, \tag{6}$$

where the subscripts $\Re$ and $\Im$ denote taking real and imaginary parts respectively. As a counterpart of $|h|$ in (3), h_R (h_I) is defined as the channel gain of transmitted $z_{\Re}$ ($z_{\Im}$). Different from (3), real and imaginary parts of z have different channel gains due to interleaving, and contain replica of a, b due to rotation. For independent identically distributed (i.i.d.) Rayleigh channels, h_R, h_I are i.i.d. Rayleigh random variables. Denoting $n_{\Re}$, $n_{\Im}$ as Gaussian noises with zero mean and $\sigma^2/2$ variance, the ML metric for detecting z is given by

$$\mathcal{M}(z) = \exp\left(-\frac{(y_{\Re} - \sqrt{E}h_Rz_{\Re})^2 + (y_{\Im} - \sqrt{E}h_Iz_{\Im})^2}{\sigma^2}\right), \tag{7}$$

and then bit likelihood ratio (LLR) can be written as

$$\mathcal{L}(i) = \ln\sum_{z\in\mathcal{A}_i^0}\mathcal{M}(z) - \ln\sum_{z\in\mathcal{A}_i^1}\mathcal{M}(z), \tag{8}$$

where $\mathcal{A}_i^l$ is a set of z whose ith bit for a particular user is l.

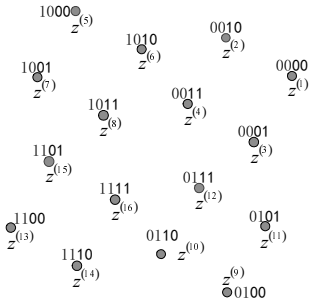

Fig. 3. Rotated composite constellation formed by QPSK.

C. Rotation angle optimization

Rotations in SSD are usually optimized by maximizing the minimum product distance or minimizing error probabilities. In [14], rotations for PSK and QAM constellations are optimized by using SER upper bounds. However, the case is quite different for NOMA constellations due to bit division between users. Assuming ML detection, SER upper bounds are derived for both users and then used for rotation angle optimization.

Denoting $z^{(i)}$ as the ith symbol of the composite constellation, SER for either near or far user can be bounded by

$$P_e \leq \frac{1}{N}\sum_{i=1}^{N}\sum_{\substack{k=1,\\ k\notin\Gamma^{(i)}}}^{N} P\left(z^{(i)}\to z^{(k)}\right), \tag{9}$$

where N is the size of the composite constellation, $P(z^{(i)}\to z^{(k)})$ is the pairwise error probability (PEP), and $\Gamma^{(i)}$ is a set of superscripts whose corresponding symbols do not constitute a valid PEP with $z^{(i)}$ for a particular user. Consider QPSK superposition in Fig. 3. For near user, no error occurs if $z^{(1)}$ is misdetected as $z^{(5)}$. This is because $z^{(1)}$, $z^{(5)}$ have the same latter two bits and both will be interpreted as "00". This type of event causes no symbol error and thus should be excluded from the summation in (9). The same applies to far user when using ML detection. For Fig. 3, $N=16$, and we have

$$\begin{aligned}
&\Gamma^{(1)}=\Gamma^{(5)}=\Gamma^{(9)}=\Gamma^{(13)}=\{1,5,9,13\},\\
&\Gamma^{(2)}=\Gamma^{(6)}=\Gamma^{(10)}=\Gamma^{(14)}=\{2,6,10,14\},\\
&\Gamma^{(3)}=\Gamma^{(7)}=\Gamma^{(11)}=\Gamma^{(15)}=\{3,7,11,15\},\\
&\Gamma^{(4)}=\Gamma^{(8)}=\Gamma^{(12)}=\Gamma^{(16)}=\{4,8,12,16\},
\end{aligned} \tag{10}$$

for near user. Similarly, we have the following for far user.

$$\begin{aligned}
&\Gamma^{(1)}=\Gamma^{(2)}=\Gamma^{(3)}=\Gamma^{(4)}=\{1,2,3,4\},\\
&\Gamma^{(5)}=\Gamma^{(6)}=\Gamma^{(7)}=\Gamma^{(8)}=\{5,6,7,8\},\\
&\Gamma^{(9)}=\Gamma^{(10)}=\Gamma^{(11)}=\Gamma^{(12)}=\{9,10,11,12\},\\
&\Gamma^{(13)}=\Gamma^{(14)}=\Gamma^{(15)}=\Gamma^{(16)}=\{13,14,15,16\}.
\end{aligned} \tag{11}$$

The PEP in (9) can be further written as

$$\begin{aligned}
&P\left(z^{(i)}\to z^{(k)}\right)=\\
&\int_0^\infty\int_0^\infty P\left(z^{(i)}\to z^{(k)}|h_R,h_I\right)p(h_R)p(h_I)dh_Rdh_I,
\end{aligned} \tag{12}$$

where i.i.d. Rayleigh channels are assumed with Rayleigh probability density functions (PDF) given as $p(h_R)$, $p(h_I)$. The conditional PEP $P(z^{(i)}\to z^{(k)}|h_R,h_I)$ can be derived as

$$\begin{aligned}
&P\left(z^{(i)}\to z^{(k)}|h_R,h_I\right)\\
&=P\Big((y_\Re-h_R\sqrt{E}z_\Re^{(k)})^2+(y_\Im-h_I\sqrt{E}z_\Im^{(k)})^2\leq\\
&\quad(y_\Re-h_R\sqrt{E}z_\Re^{(i)})^2+(y_\Im-h_I\sqrt{E}z_\Im^{(i)})^2|z^{(i)}\text{sent}\Big) &(13)\\
&=P\Big(h_R(z_\Re^{(i)}-z_\Re^{(k)})n_\Re+h_I(z_\Im^{(i)}-z_\Im^{(k)})n_\Im\leq\\
&\quad-\frac{1}{2}\sqrt{E}h_R^2(z_\Re^{(i)}-z_\Re^{(k)})^2-\frac{1}{2}\sqrt{E}h_I^2(z_\Im^{(i)}-z_\Im^{(k)})^2\Big) &(14)\\
&=\frac{1}{2}\text{erfc}\left(\frac{1}{2}\sqrt{\frac{E}{\sigma^2}}\sqrt{h_R^2(z_\Re^{(i)}-z_\Re^{(k)})^2+h_I^2(z_\Im^{(i)}-z_\Im^{(k)})^2}\right) &(15)\\
&\leq\frac{1}{2}\exp\left(-\frac{E}{4\sigma^2}\left(h_R^2(z_\Re^{(i)}-z_\Re^{(k)})^2+h_I^2(z_\Im^{(i)}-z_\Im^{(k)})^2\right)\right). &(16)
\end{aligned}$$

(13) follows the conditional PEP definition. (14) is obtained by substituting (5), (6) into (13). As $h_R(z_\Re^{(i)}-z_\Re^{(k)})n_\Re+h_I(z_\Im^{(i)}-z_\Im^{(k)})n_\Im$ in (14) is a Gaussian random variable with computable mean and variance, (15) can be derived by using the equality $P(X\leq -x)=\frac{1}{2}\text{erfc}\left(\sqrt{x^2/2\Omega^2}\right)$ where X is a Gaussian random variable with zero mean and Ω^2 variance. (16) is obtained by using the inequality $\text{erfc}(x)\leq e^{-x^2}$ and is a function of h_R^2, h_I^2. Substituting (16) into (12), (12) can be calculated as scaled by an integral w.r.t. h_R^2, h_I^2. The required $p(h_R^2)$, $p(h_I^2)$ can be easily obtained considering $p(x^2)=e^{-x^2}$ holds for Rayleigh PDF $p(x)$. Thereby, (12) can be scaled as

$$\begin{aligned}
&P\left(z^{(i)}\to z^{(k)}\right)\\
&\leq\frac{1}{2}\int_0^\infty\exp\left(-h_R^2\left(1+\frac{E}{4\sigma^2}(z_\Re^{(i)}-z_\Re^{(k)})^2\right)\right)dh_R^2\\
&\quad\times\int_0^\infty\exp\left(-h_I^2\left(1+\frac{E}{4\sigma^2}(z_\Im^{(i)}-z_\Im^{(k)})^2\right)\right)dh_I^2\\
&=\frac{1}{2\left(1+\frac{\left(z_\Re^{(i)}-z_\Re^{(k)}\right)^2E}{4\sigma^2}\right)\left(1+\frac{\left(z_\Im^{(i)}-z_\Im^{(k)}\right)^2E}{4\sigma^2}\right)}.
\end{aligned} \tag{17}$$

Substituting (17) into (9), finally we have

$$\begin{aligned}
&P_e\leq U(\theta_a,\theta_b)=\\
&\frac{1}{2N}\sum_{i=1}^{N}\sum_{\substack{k=1,\\ k\notin\Gamma^{(i)}}}^{N}\frac{1}{\left(1+\frac{\left(z_\Re^{(i)}-z_\Re^{(k)}\right)^2E}{4\sigma^2}\right)\left(1+\frac{\left(z_\Im^{(i)}-z_\Im^{(k)}\right)^2E}{4\sigma^2}\right)}.
\end{aligned} \tag{18}$$

As z is a function of θ_a, θ_b, so is the SER upper bound $U(\theta_a,\theta_b)$ in (18). Note that $U(\theta_a,\theta_b)$ is a universal formulation. To get the SER upper bound for near or far user, user-

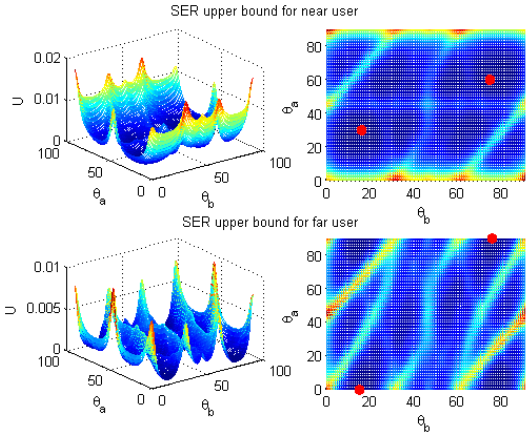

Fig. 4. One example for SER upper bounds of near and far users.

specific σ^2 and $\Gamma^{(i)}$ should be used in $U(\theta_a, \theta_b)$. Rotation angles are optimized by minimizing $U(\theta_a, \theta_b)$, i.e.,

$$(\theta_a^*, \theta_b^*) = \arg \min_{\theta_a, \theta_b} U(\theta_a, \theta_b), \tag{19}$$

The optimization can be performed towards either near or far user by using its corresponding $U(\theta_a, \theta_b)$. To solve the non-convex problem, a numerical method is used by performing a global search with a step of 1°. As obvious discrepancy of $U(\theta_a, \theta_b)$ v.s. SNR curves appears in high SNR, E/σ^2 can be set to a relatively large value. Assuming power ratio $\rho_a/\rho_b = 1/4$ and QPSK, $U(\theta_a, \theta_b)$ for both users are illustrated in Fig. 4, where red points indicate optimal rotation angles. We choose $\theta_a^* = 30^\circ$, $\theta_b^* = 16^\circ$ for near user optimization, and $\theta_a^* = 0^\circ$, $\theta_b^* = 15^\circ$ for far user optimization. Here only QPSK superposition is exemplified, while the methodology is generally applicable to other constellation combinations.

IV. Simulation Results

In this section, link-level simulations are given for a LTE system with 10MHz bandwidth. Power ratios $\rho_a = 0.2$, $\rho_b = 0.8$ and QPSK modulation are assumed. Six physical resource block pairs are used for downlink NOMA, where the overhead consists of 3-symbol physical downlink control channel, 2-port cell-specific reference signal and 4-port demodulation reference signal. The evaluated schemes include conventional NOMA, Gray-mapping NOMA and the proposed methods with rotation optimized for near and far users (abbreviated as "Opt for near" and "Opt for far" respectively). For all the schemes, ML detection is used for both users. Rotation angles are $\theta_a^* = 30^\circ$, $\theta_b^* = 16^\circ$ for the method "Opt for near", and $\theta_a^* = 0^\circ$, $\theta_b^* = 15^\circ$ for the method "Opt for far". SNR is defined as the ratio of total power to user-specific noise power. Other parameters can be found in Table I.

To verify the effectiveness of rotation, Fig. 5 shows SER performance of each user under i.i.d. Rayleigh channels. For Gray-mapping NOMA, near user performs a little better, but far user performs the same compared with conventional NOMA. This is because Gray mapping has no impact on far

TABLE I
Simulation Parameters

Parameter	Assumption
Antenna configuration	1 Tx, 1Rx
MCS level	MCS = 9 (QPSK) for both users
Channel coding	Turbo coding in LTE
Channel estimation	Ideal
SNR definition	near user: E/σ^2_{near}; far user: E/σ^2_{far}

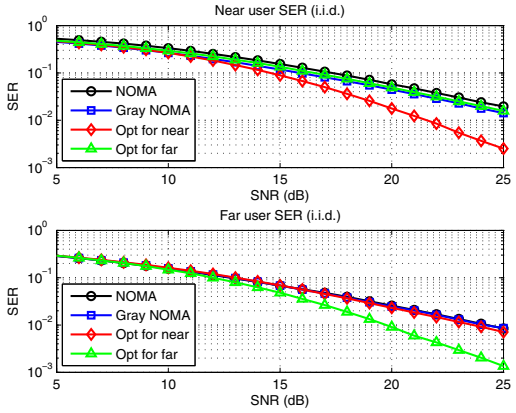

Fig. 5. SER for different NOMA schemes, i.i.d. Rayleigh channel.

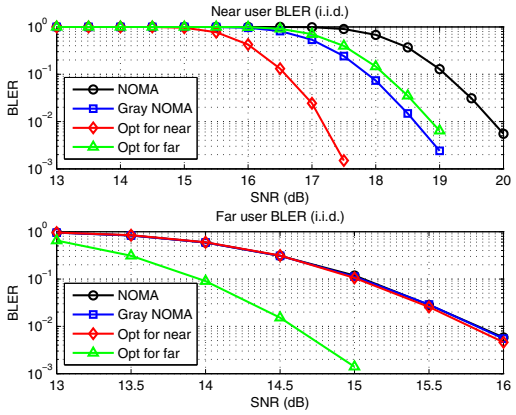

Fig. 6. BLER for different NOMA schemes, i.i.d. Rayleigh channel.

user posterior probability calculation. For the method "Opt for near", a relatively large gain can be observed for near user and far user performs similarly compared with Gray-mapping NOMA. Comparing the method "Opt for far" with Gray-mapping NOMA, far user enjoys a relatively large gain, and performance loss is observed for near user but only marginal.

As a more meaningful performance indicator, block error rate (BLER) is evaluated next. From Fig. 5, the gain usually comes at a relatively high SNR. Thereby, a relatively high code rate is used to evaluate the potential BLER gain. Given modulation and coding scheme (MCS) level 9, the code rate is about 0.8. BLER performance under i.i.d. Rayleigh channels is given in Fig. 6. Still Gray-mapping NOMA outperforms conventional NOMA w.r.t. near user, but performs the same

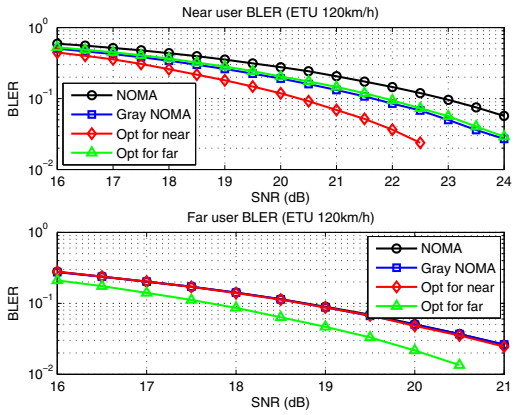

Fig. 7. BLER for different NOMA schemes, ETU 120km/h channel.

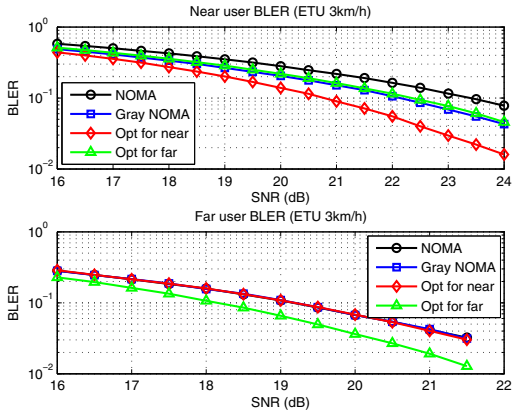

Fig. 8. BLER for different NOMA schemes, ETU 3km/h channel.

for far user. Comparing the method "Opt for near" with Gray-mapping NOMA, about 1.3 dB gain at 0.1 BLER can be observed for near user, and there is no performance loss for far user. Comparing the method "Opt for far" with Gray-mapping NOMA, far user has about 1 dB gain at 0.1 BLER, and near user performs slightly worse, i.e., enduring about 0.2 dB loss. The degradation is because optimization does not consider impact on the other user. According to simulations, performance loss is usually marginal. This paper targets the best performance a particular user can achieve, while tradeoff between different users is left for future study.

BLER under other types of channels are also evaluated. Simulation results for extended typical urban (ETU) channels with speeds 120 km/h and 3 km/h are given in Fig. 7 and Fig. 8 respectively. Similar observations can be obtained for both channels when compared with Gray-mapping NOMA. When rotation optimization is towards near user, the performance of near user is enhanced by about 1.3 dB at 0.1 BLER, while there is no performance loss for far user. When rotation optimization is towards far user, far user has about 1 dB gain at 0.1 BLER, while near user performs almost the same as that of Gray-mapping NOMA.

From Fig. 7, 8 and simulations under various other channels which are not shown due to space constraints, the gain which comes from diversity is obvious when the channel is more close to an i.i.d. channel, such as a frequency selective or fast fading channel. In contrast, the diversity gain tends to diminish when the channel is more like an additive white Gaussian noise (AWGN) channel, such as a flat and slow fading channel. In an extreme case, there will be no diversity gain in the AWGN channel, which coincides with intuitions. The practical gain for a real-life system depends on integrated effects of channel variation, power allocation, user scheduling, modulation adaptation and antenna configuration. This will be evaluated with system-level simulations in our future work.

V. Conclusion

In this paper, a method of NOMA constellation rotation is proposed to exploit signal space diversity for downlink NOMA. To preserve full degrees of freedom, two independent angles are used to rotate NOMA superposed constellations respectively. Assuming ML detection, the SER upper bounds for both near and far users are derived and used for rotation angle optimization. With the target of revealing the best performance a particular user can achieve, rotation optimization can be performed towards either near user or far user. Simulation results show that there is diversity gain for the optimized user while almost no performance loss for the other user.

References

[1] ITU, "IMT Vision - Framework and overall objectives of the future development of IMT for 2020 and beyond," June 2015.

[2] A. Goldsmith, *Wireless Communications*. Cambridge University Press, 2005.

[3] Y. Saito, Y. Kishiyama, A. Benjebbour, T. Nakamura, A. Li, and K. Higuchi, "Non-orthogonal multiple access (NOMA) for future radio access," *IEEE VTC Spring 2013*, June 2013.

[4] C. Yan, A. Harada, A. Benjebbour, Y. Lan, A. Li and H. Jiang, "Receiver design for downlink non-orthogonal multiple access (NOMA)," *IEEE VTC Spring 2015*, May 2015.

[5] 3GPP R1-154184, "Bit to symbol mapping for multiuser superposition transmission," Samsung, Aug. 24-Aug. 28, 2015.

[6] 3GPP R1-154055, "Potential transmission schemes for MUST," ZTE, Aug. 24-Aug. 28, 2015.

[7] 3GPP TR-36.859 (V13.0.0), 3rd Generation Partnership Project; Technical Specification Group Radio Access Network; Study on Downlink Multiuser Superposition Transmission (MUST) for LTE (Release 13).

[8] T. Yazaki and Y. Sanada, "Effect of joint detection and decoding in non-orthogonal multiple access," *IEEE ISPACS 2014*, Dec. 2014.

[9] T. Seyama, T. Dateki and H. Seki, "Efficient selection of user sets for downlink non-orthogonal multiple access," *IEEE PIMRC 2015*, Sept. 2015.

[10] M. -R. Hojeij, J. Farah, C. A. Nour and C. Douillard, "Resource allocation in downlink non-orthogonal multiple access (NOMA) for future radio access," *IEEE VTC Spring 2015*, May 2015.

[11] K. Higuchi and Y. Kishiyama, "Non-orthogonal access with random beamforming and intra-beam SIC for cellular MIMO downlink," *IEEE VTC Fall 2013*, Sept. 2013.

[12] Yue Tian, Shani Lu, A. Nix and M. Beach, "A novel opportunistic NOMA in downlink coordinated multi-point networks," *IEEE VTC Fall 2015*, Sept. 2015.

[13] J. Boutros and E. Viterbo, "Signal space diversity: a power and bandwidth efficient diversity technique for the Rayleigh fading channel," *IEEE Trans. Inform. Theory*, vol. 44, no. 4, pp. 1453-1467, July 1998.

[14] M. N. Khormuji, U. H. Rizvi, G. J. Janssen, and S. B. Slimane, "Rotation optimization for MPSK/MQAM signal constellations over Rayleigh fading channels," *IEEE ICCS 2006*, Oct. 2006.